Contribution from the Department of Chemistry,
Faculty of Science, Kyushu University, Higashiku, Fukuoka 812, Japan

Rapid Electronic Relaxation Phenomenon in a $^2T \rightleftarrows {}^6A$ Spin-Equilibrium System

HIROKI OHSHIO,† YONEZO MAEDA,* and YOSHIMASA TAKASHIMA

Received December 3, 1982

The magnetic susceptibilities, Mössbauer spectra, and electron paramagnetic resonance (EPR) spectra of [Fe(acen)(dpp)](BPh_4), [Fe(acen)(pic)$_2$](BPh_4), and [Fe(acen)(lut)$_2$](BPh_4) have been measured in the solid state [acen = *N*,*N*'-bis(1-methyl-3-oxobutylidene)ethylenediamine, dpp = 1,3-di-4-pyridylpropane, pic = 4-methylpyridine, lut = 3,4-dimethylpyridine, and BPh_4 = tetraphenylborate ion]. The variable-temperature magnetic susceptibility for these complexes has been interpreted by the spin-crossover phenomenon between ^6A and ^2T states. The EPR parameters for the ^2T state have been used to determine the energy levels of three Kramers doublets. The temperature dependence of the Mössbauer spectra for [Fe(acen)(dpp)](BPh_4) and [Fe(acen)(pic)$_2$](BPh_4) has proved the existence of rapid electronic relaxation between two spin states in comparison with the Mössbauer lifetime of 0.97×10^{-7} s. The separation energies between the two spin states have been estimated to be 330 and 339 cm^{-1} for [Fe(acen)(dpp)](BPh_4) and [Fe(acen)(pic)$_2$](BPh_4), respectively, by the theoretical calculation of the temperature dependence of the quadrupole splittings.

Introduction

Iron(II) and iron(III) complexes exhibit a temperature-dependent spin transition (so-called spin crossover), if the ligand field strength is comparable to the mean spin-pairing energy.

The spin transition takes place between ^1A and ^5T states in spin-crossover iron(II) complexes, and these spin states are reflected by distinct resonances in the Mössbauer spectrum if the complexes are characterized by a slow electronic relaxation between the two spin states relative to the lifetime of the nuclear excited state of iron-57.[1] König et al. determined the Debye–Waller factors $f(^5T)$ and $f(^1A)$ of many spin-crossover iron(II) complexes.[2-6] These results have shown that different lattice dynamic properties exist between the states of ^5T and ^1A because of the discontinuity of the Debye–Waller factor at the temperature of spin transition. Recently, they proposed a model for the spin transition in the solid state including the effect of a low-symmetry ligand field and spin–orbit coupling and explained the temperature dependence of the magnetic susceptibilities by taking into account the interaction between ferrous ions in using an Ising Hamiltonian.[7] Sorai and Seki suggested that there is a significant coupling between an electronic state and a phonon system and a spin transition occurs in a cooperative region (so-called domain).[8,9] In this respect, Gütlich et al. proposed that the spin transition takes place through a cooperative coupling between the electronic states and intermolecular vibration.[10,11]

On the other hand, the spin crossover of iron(III) (^6A–^2T) has been known in the case of the *N*,*N*-dialkyldithiocarbamate.[12,13] Rickards et al. recorded the Mössbauer spectra of *N*,*N*-dialkyldithiocarbamate at various temperatures and reported that a poorly resolved doublet was only observed above 78 K.[14] This result shows that a rapid electronic relaxation occurs between the ^6A and ^2T states in comparison to the Mössbauer lifetime; therefore, the Mössbauer spectra are averaged and depend on the population of the ^6A and ^2T states at the temperature of measurement. Recently, another example was reported to have rapid electronic relaxation between ^6A and ^2T.[15-20]

In the present study, new spin-crossover iron(III) complexes that show rapid electronic relaxation between the ^6A and ^2T states compared with the lifetime of the nuclear excited state of iron-57 were studied by means of Mössbauer spectroscopy, EPR spectra, and magnetic susceptibility measurements.

Experimental Section

(a) Sample Preparation. The quadridentate Schiff base (acen) used in this study was prepared according to the method of Holm.[21] [Fe(acen)(dpp)](BPh_4) was prepared by adding 1,3-di-4-pyridylpropane in 10 mL of absolute methanol to the [Fe(acen)Cl] (0.1 mmol) in 30 mL of absolute methanol. This solution was refluxed for 10 min, and after filtration sodium tetraphenylborate (0.1 mmol) in 10 mL of methanol was slowly added. The blue-black polycrystallines were filtered with suction and washed with cold methanol. Anal. Calcd for $FeC_{49}H_{52}N_4O_2B$: C, 73.97; H, 6.59; N, 7.04. Found: C, 73.70; H, 6.80; N, 6.88. [Fe(acen)(pic)$_2$](BPh_4) has been prepared by Kida et al.[22] This complex was prepared in the same manner as the above complex except that 4-methylpyridine was used. Anal. Calcd for $FeC_{48}H_{55}N_4O_2B$: C, 73.57; H, 6.68; N, 7.15. Found: C, 73.43; H, 6.62; N, 7.10. [Fe(acen)(lut)$_2$](BPh_4) was prepared in the same manner as the above complex except that 3,4-lutidine was used. Anal. Calcd for $FeC_{50}H_{56}N_4O_2B$: C, 73.99; H, 6.95; N, 6.90. Found: C, 73.43; H, 6.62; N, 7.10.

(b) Physical Measurements. Magnetic susceptibilities on the polycrystalline samples were measured by the Faraday method using an electrobalance, Type 2002, (Cahn Instrument) with an electromagnet (8000 G) operated at 20 A. The temperature was controlled over 78–300 K by using a digital temperature controller, Model 3700 (Scientific Instruments). $HgCo(NCS)_4$ was used as a calibration substance. The effective magnetic moment was calculated by the formula $\mu_{eff} = 2.84(\chi_M T)^{1/2}$, where χ_M is a molar susceptibility after applying diamagnetic correction.

† Present address: Todd Wehr Chemistry, Marquette University, Milwaukee, WI 53233.

(1) Maeda, Y.; Takashima, Y.; Nishida, Y. Bull. *Chem. Soc. Jpn.* **1976**, *49*, 2427.
(2) König, E.; Ritter, G.; Spiering, H.; Kremer, S. *J. Chem. Phys.* **1972**, *56*, 3139.
(3) König, E.; Ritter, G.; Goodwin, H. A. *Chem. Phys.* **1973**, *1*, 17.
(4) König, E.; Ritter, G. *Phys. Lett. A* **1973**, *43A*, 488.
(5) König, E.; Ritter, G.; Goodwin, H. A. *Chem. Phys.* **1974**, *5*, 211.
(6) König, E.; Ritter, G.; Irler, W.; Goodwin, H. A.; Kanellakopulos, B. *J. Phys. Chem. Solids* **1977**, *39*, 521.
(7) Zimmermann, R.; König, E. *J. Phys. Chem. Solids* **1977**, *38*, 779.
(8) Sorai, M.; Seki, S. *J. Phys. Soc. Jpn.* **1972**, *33*, 575.
(9) Sorai, M.; Seki, S. *J. Phys. Chem. Solids* **1974**, *35*, 555.
(10) Sorai, M.; Ensling, J.; Gütlich, P. *Chem. Phys.* **1976**, *18*, 199.
(11) Sorai, M.; Ensling, J.; Hasselbach, K. M.; Gütlich, P. *Chem. Phys.* **1977**, *20*, 197.
(12) Frank, E.; Abeledo, C. R. *Inorg. Chem.* **1966**, *5*, 1453.
(13) Cambi, L.; Szego, L. *Ber. Dtsch. Chem. Ges. B* **1931**, *64*, 2591.
(14) Rickards, R.; Johnson, C. E.; Hill, H. A. O. *J. Chem. Phys.* **1968**, *48*, 5231.
(15) Cox, M.; Darken, J.; Fitzsimmons, B. W.; Smith, A. W.; Larkorthy, L. F.; Rogers, K. A. *J. Chem. Soc., Dalton Trans.* **1972**, 1192.
(16) Tweedle, M. F.; Wilson, L. J. *J. Am. Chem. Soc.* **1976**, *98*, 4824.
(17) Sinn, E.; Sim, G.; Dose, E. V.; Tweedle, M. F.; Wilson, L. J. *J. Am. Chem. Soc.* **1978**, *100*, 3375.
(18) Petty, R. H.; Dose, E. V.; Tweedle, M. F.; Wilson, L. J. *Inorg. Chem.* **1978**, *17*, 1064.
(19) Hodges, K. D.; Wollmann, R. G.; Kessel, S. L.; Hendrickson, D. N.; Van Derveer, D. G.; Barefield, E. K. *J. Am. Chem. Soc.* **1979**, *101*, 906.
(20) Haddad, M. S.; Federer, W. D.; Lynch, M. W.; Hendrickson, D. N. *Inorg. Chem.* **1981**, *20*, 131.
(21) Holm, R. H.; Everett, G. W.; Charkravorty, A. *Prog. Inorg. Chem.* **1965**, *7*, 83.
(22) Nishida, Y.; Oshio, S.; Kida, S. *Bull. Chem. Soc. Jpn.* **1977**, *50*, 119.

0020-1669/83/1322-2684$01.50/0

Table I. Changes of the Thermodynamic Data and the Crossover Parameters of Iron(III) Complexes

complex	ΔH,[a] cal mol^{-1}	ΔS,[b] eu	E,[c] cm^{-1}	g[d]	log C[e]	ζ,[f] cm^{-1}
[Fe(acen)(dpp)](BPh$_4$)	2122	11	536	2.14	1.88	163
[Fe(acen)(γ-pic)$_2$](BPh$_4$)	2880	12	652	2.14	2.19	360
[Fe(acen)(3,4-lut)$_2$](BPh$_4$)	2688	12	528	2.13	2.18	430

[a] Changes of the enthalpy for the spin transition. [b] Changes of the entropy for the spin transition. [c] Separation between zero-point levels of the low- and high-spin states. [d] The g value obtained from EPR spectrum at 80 K. [e] C = ratio of the molecular partition functions in the two states. [f] One-electron spin-orbit coupling constant.

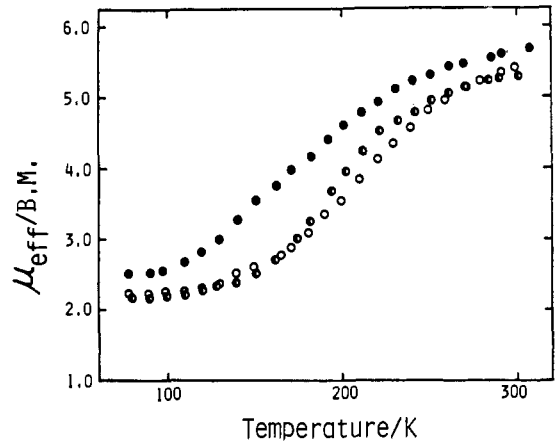

Figure 1. Temperature dependence of the effective magnetic moments for [Fe(acen)(dpp)](BPh$_4$) (●), [Fe(acen)(pic)$_2$](BPh$_4$) (◐), and [Fe(acen)(lut)$_2$](BPh$_4$) (○).

Electron paramagnetic resonance spectra on the polycrystalline samples were recorded by using a JEX-FEX (JEOL, Ltd.) X-band spectrometer. The magnetic field was calibrated with a 2,2-diphenyl-1-picrylhydrazyl.

Mössbauer spectra were measured with a constant-acceleration spectrometer (Austin Science Associates (ASA)). Data were stored in a 1024-channel pulse height analyzer, Type 5200 (Inotech, Inc). The temperature was monitored with a calibrated copper vs. constantan thermocouple within a variable-temperature cryostat, Type ASAD-4V (ASA). A cobalt-57 source of 10 mCi diffused into a palladium foil was used for the absorption measurement. All the spectra were fitted to the Lorentzian line shape by using the least-squares method at the Computer Center, Kyushu University, and the velocity scale was normalized with respect to the center of the spectrum of metallic iron at 297 K.

Results and Discussion

(a) Magnetic Susceptibility. The variable-temperature magnetochemical data in the 78–307 K range for the complexes are shown in Figure 1. The values of the effective magnetic moment for the three complexes increase gradually from ca. 2.3 μ_B at 80 K to ca 5.6 μ_B at room temperature and exhibit non-Curie behavior typical of a $^6A \rightleftarrows {}^2T$ spin-equilibrium process. The high-spin population (x) at a certain temperature is obtained by assuming a simple additive property in magnetic susceptibilities, and the equilibrium constant can be obtained by $K = x/(1 - x)$. The changes of the enthalpy (ΔH) and entropy (ΔS) accompanying the spin transition are evaluated by using the equation $\ln K = -\Delta H/RT + \Delta S/R$, and the kinetic data obtained are listed in Table I. The entropy changes accompanying the spin transition are 5 times as large as the values expected from the magnetic contribution of the $^6A \rightleftarrows {}^2T$ process ($R \ln 3 = 9.1$ J K^{-1} mol^{-1}). This shows that the lattice vibrations of the complexes play an important role in the spin transition.[23] This is consistent with the result of the temperature dependence of the area under the Mössbauer resonance line, as discussed below. There is no difference in the values of the enthalpy changes between

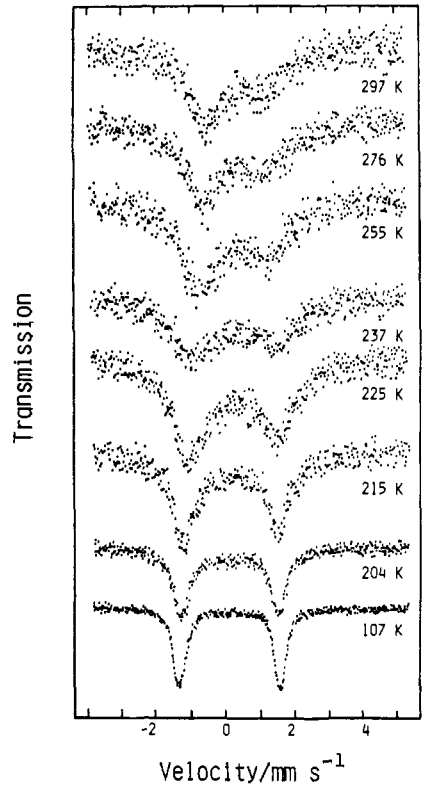

Figure 2. Mössbauer spectra of [Fe(acen)(pic)$_2$](BPh$_4$) at various temperatures.

[Fe(acen)(dpp)](BPh$_4$) (rapid spin-interconversion system) and [Fe(acen)(lut)$_2$](BPh$_4$) (slow spin-interconversion system).

The separation energy (E) between zero-point levels of the low- and high-spin states is estimated from the temperature dependence of the molecular vibrational partition functions between the two spin states:[24]

$$\mu_{eff}^2 = \{0.75g^2 + 8x^{-1}[1 - \exp(-3x/2)] + 105C \exp[-(1 + E/\zeta)x]\}/\{1 + 2\exp(-3x/2) + 3C \exp[-(1 + E/\zeta)x]\}$$

where ζ is the one-electron spin–orbit coupling constant and $x = \zeta/kT$. The value of log C was evaluated from the equilibrium constant and the experimental g value obtained from EPR data. The best-fit parameters for the complexes calculated by the least-squares method are summarized in Table I.

(b) Mössbauer Spectra: [Fe(acen)(dpp)](BPh$_4$) and Fe[(acen)(pic)$_2$](BPh$_4$). The Mössbauer spectra for [Fe(acen)(pic)$_2$](BPh$_4$) at various temperatures are shown in Figure 2. The statistics of the spectra are very poor at high temperature due to a very low Debye–Waller factor (the absorption is ~1%). The Mössbauer spectra for [Fe(acen)(dpp)](BPh$_4$) are not shown because they are quite similar to those for [Fe(acen)(pic)$_2$](BPh$_4$). The quadrupole doublet with the narrow full width at half-maximum (fwhm) appearing at 107 K (Figure 2) is ascribed to a low-spin iron(III), and

(23) Ewald, A.; Martin, R. L.; Ross, I. G.; White, A. H. *Proc. R. Soc. London, Ser. A* **1964**, *280*, 235.

(24) Ewald, A.; Martin, R. L.; Sinn, E.; White, A. H. *Inorg. Chem.* **1969**, *8*, 1837.

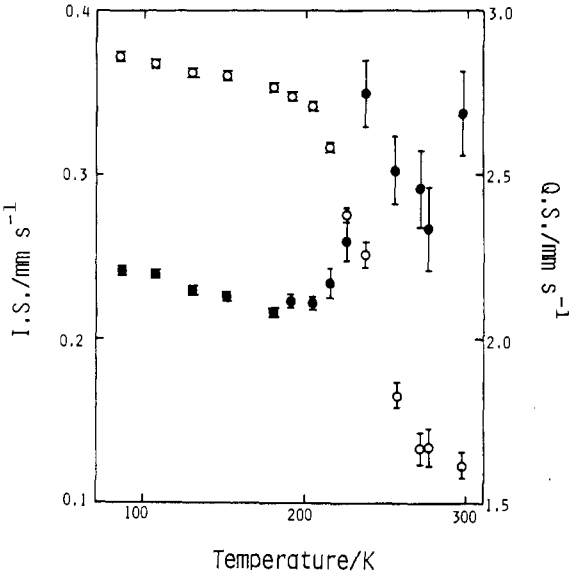

Figure 3. Temperature dependence of the isomer shift (●) and quadrupole splitting (○) for [Fe(acen)(pic)$_2$](BPh$_4$).

the resonance lines corresponding to a high-spin iron(III) are observed in the spectra at 297 K. The spectra were legitimately analyzed as a doublet. The increase of the quadrupole splitting apears to be parallel with an increase of the ^{2}T low-spin isomer population as the temperature is lowered. One could expect to find a superposition of the quadrupole doublets of two spin states between the intermediate temperature ranges; however, only one quadruple doublet with a broad line width is observed in this temperature range. This phenomenon indicates that the relaxation time to change from low-spin state to high-spin state and vice versa is shorter than the lifetime of the excited Mössbauer nuclear state and that the nucleus sees an "average" of the electronic states of high- and low-spin states. Namely, the spectra of these complexes show a rapid electronic relaxation phenomenon between the two states.[25-27]

The temperature dependence of the isomer shift exhibits the typical behavior of a low-spin iron(III) state between 87 and 180 K (Figure 3): It is reasonable to expect that the value of the isomer shift increases with decreasing temperature for spin-invariant complexes because of the temperature dependence of the second-order Doppler shift. However, the values change drastically up to the values characteristic of a high-spin iron(III) in the temperature range between 192 and 237 K, and the values in the temperature range of spin transition are intermediate between those of two spin states and change with the population of high- (or low-) spin states.

The temperature dependence of the recoil-free fraction provides information about the lattice dynamic properties of the solid state accompanying the motion of a Mössbauer atom. The recoil-free fraction can be calculated by applying the Debye model. In a thin absorber approximation, the temperature dependence of the recoil-free fractions can be given by the temperature dependence of the area under the resonance curve. The Debye model approximation leads to $\mathrm{d} \ln f/\mathrm{d}T \propto \mathrm{d} \ln A/\mathrm{d}T$ in the high-temperature limit. The plots of ln $[A(T)/A(107)]$ vs. temperature (Figure 4) show a discontinuity in the temperature range of 192–215 K, which suggests that some kind of phase transition occurs in this temperature range: The spin transition accompanies the change of the intermolecular or lattice vibration.

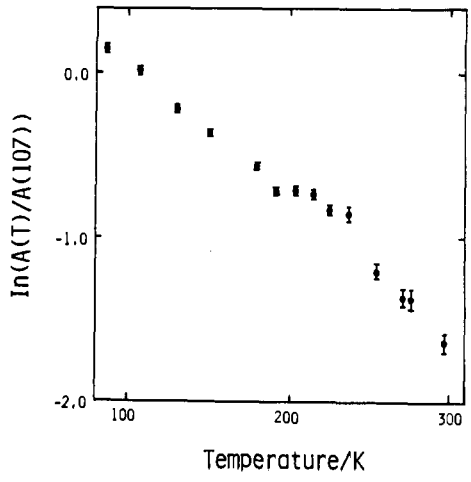

Figure 4. Temperature dependence of the area under the Mössbauer resonance line for [Fe(acen)(pic)$_2$](BPh$_4$).

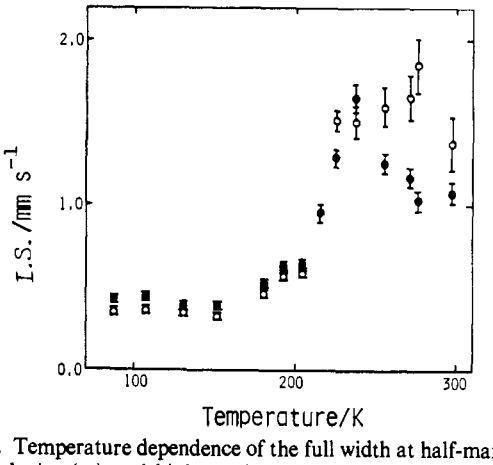

Figure 5. Temperature dependence of the full width at half-maximum (lower velocity (●) and higher velocity (○)) for [Fe(acen)(pic)$_2$]-(BPh$_4$).

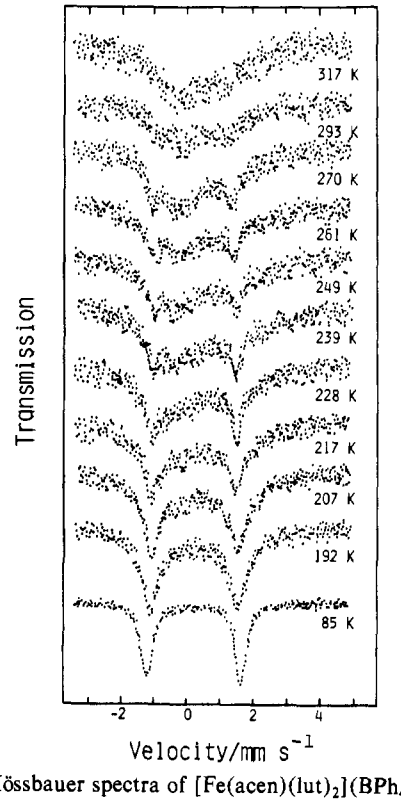

Figure 6. Mössbauer spectra of [Fe(acen)(lut)$_2$](BPh$_4$) at various temperatures.

(25) Epstein, L. M.; Straub, D. K. *Inorg. Chem.* **1969**, *8*, 784.
(26) Eibschütz, M.; Lines, M. E.; DiSalvo, F. J. *Phys. Rev. B: Condens. Matter* **1977**, *15*, 103.
(27) Maeda, Y.; Tsutsumi, N.; Takashima, Y. *Chem. Phys. Lett.* **1982**, *88*, 248.

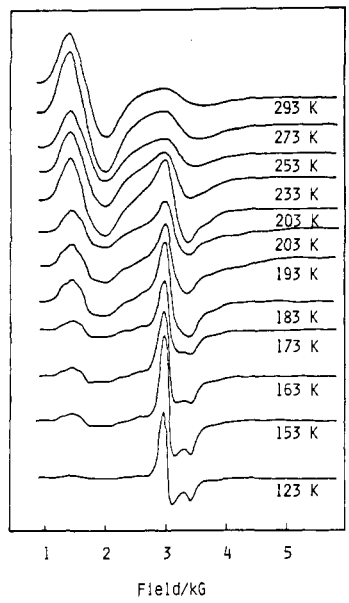

Figure 7. EPR spectra of [Fe(acen)(dpp)](BPh_4) at various temperatures.

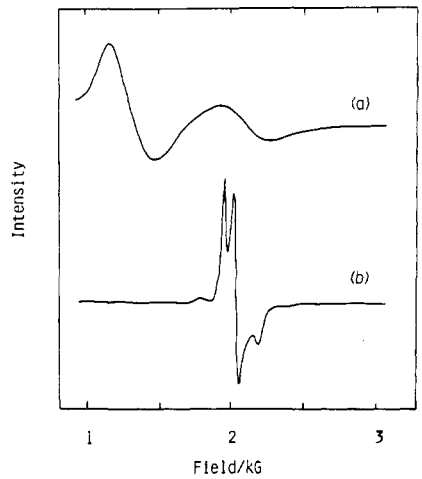

Figure 8. EPR spectra of [Fe(acen)($pic)_2$](BPh_4) at (a) 297 K and (b) 80 K.

The increase of the fwhm values (Figure 5) results in the fact that the electronic relaxation time between the two spin states is comparable to the lifetime of the excited Mössbauer nuclear state as the temperature is raised from 180 to 237 K.

[Fe(acen)(lut)$_2$](BPh$_4$). The Mössbauer spectra of [Fe(acen)($lut)_2$](BPh_4) at various temperatures are shown in Figure 6. A quadrupole doublet ascribed to a low-spin iron(III) appears in the spectra below 173 K. On the other hand, the Mössbauer spectra above 192 K are composed of two quadrupole doublets corresponding to low- and high-spin states. The existence of two kinds of doublets becomes clear in the spin-transition temperature range (239 and 293 K). The electronic relaxation time in the spin transition of [Fe(acen)($lut)_2$](BPh_4) is longer than the Mössbauer lifetime. The decrease of spin-interconversion rate of this complex as compared with the case of the other two complexes may result from the steric structure. Namely, the additional methyl group bonded to the pyridine ring may hinder the motion of the ligand accompanied with the spin transition.

The Mössbauer parameters were not able to obtain above 192 K because of the line broadening due to the paramagnetic relaxation of the high-spin iron(III) state or maybe to a slow electronic relaxation between ^6A and ^2T spin states.

(c) EPR Spectra. EPR is a useful tool in the study of the electronic state of the spin-crossover system if the spin-lattice relaxation is not so rapid that it is difficult to obtain signals. The effect of molecular distortion and spin–orbit coupling interaction split the ^2T state into three Kramers doublets. The high-spin ^6A state also splits into three Kramers doublets, though their splittings are very small. Figures 7–9 show the EPR spectra at 297 and 80 K for polycrystalline samples of [Fe(acen)(dpp)](BPh_4), [Fe(acen)($pic)_2$](BPh_4), and [Fe(acen)($lut)_2$](BPh_4). The temperature profiles of the EPR spectra of the above three complexes are similar to each other. Two EPR signals are observed at 297 K, one at g = ca. 4.1 and the other at g = ca. 2.1. The presence of the g = ca. 4.1 signal for high-spin iron(III) indicates that the molecular symmetry is low (rhombic). As the temperature is lowered,

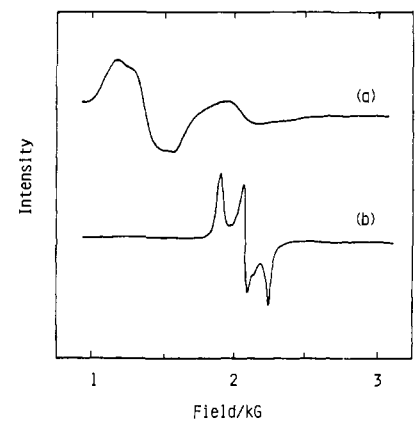

Figure 9. EPR spectra of [Fe(acen)($lut)_2$](BPh_4) at (a) 297 K and (b) 80 K.

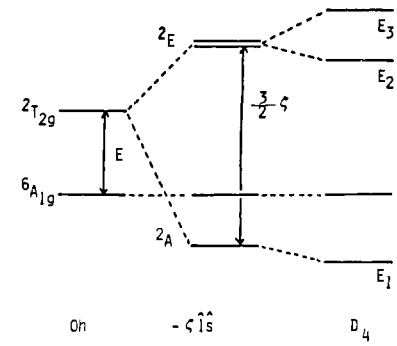

Figure 10. Energy level diagram for the spin-crossover iron(III) system: O_h crystal field (O_h symmetry) interaction; $-\zeta\hat{l}\hat{s}$, spin-orbital coupling interaction; D_4, tetragonal distortion (from O_h symmetry) interaction.

Table II. Experimental and Calculated EPR Parameters

	dpp[a]	γ-pic[b]	3,4-lut[c]
g_x	2.269	2.296	2.389
g_y	2.226	2.194	2.130
g_z	1.938	1.942	1.901
δ/ζ	2.35	2.43	2.55
ϵ/ζ	−0.17	−0.42	−1.04
A_1	0.107	0.106	0.115
B_1	0.995	0.995	0.990
C_1	−0.007	−0.017	−0.043
E_1/ζ	−4.775	−4.937	−5.173
A_2	0.908	0.814	0.750
B_2	−0.100	−0.096	−0.117
C_2	−0.406	−0.572	−0.651
E_2/ζ	1.697	1.121	0.545
A_3	0.405	0.577	0.651
B_3	−0.037	−0.047	−0.045
C_3	−0.914	−0.829	−0.758
E_3/ζ	3.078	3.816	5.719

[a] [Fe(acen)(dpp)](BPh_4). [b] [Fe(acen)(γ-$pic)_2$](BPh_4). [c] [Fe(acen)(3,4-$lut)_2$](BPh_4).

the g = ca. 2.1 signal splits into three components. Experimental anisotropic g values for the low-spin state of the three complexes are listed in Table II.

Figure 10 gives the energy level diagram for a spin-crossover iron(III) complex. We elucidated the nature of the ground-state Kramers doublet of the ^2T of pseudooctahedral iron(III) complexes by using the anisotropic g values. In this calculation the spin–orbit coupling interactions and the crystal field distortions are considered. Considering the $(t_2)^5$ configuration as a $(t_2)^1$ configuration, the six spin–orbit distortion matrix eigenfunctions may be given as[28]

$$\phi_i^+ = A_i|1^+\rangle + B_i|\zeta_1^-\rangle + C_i|-1^+\rangle$$

$$\phi_i^- = A_i|-1^-\rangle - B_i|\zeta_1^+\rangle + C_i|1^-\rangle$$

$$i = 1, 2, 3 \qquad \zeta_1 = \frac{1}{2^{1/2}}(|2\rangle - |-2\rangle)$$

The Kramers doublet will split by the magnetic field interaction, and if we consider the covalency effect, the magnetic field interaction will be given by $\mathcal{H} = \beta(k\mathbf{l} + 2\mathbf{s})H$, where k is the orbital reduction factor. By considering the matrix elements of $k\mathbf{l}_z + 2\mathbf{s}_z$, $k\mathbf{l}_x + 2\mathbf{s}_x$, and $k\mathbf{l}_y + 2\mathbf{s}_y$, we find each g value for the ground-state level as

$$g_z = 2[A^2 - B^2 + C^2 + k(A^2 - C^2)]$$

$$g_x = 2[B^2 - 2AC + 2^{1/2}kB(A - C)]$$

$$g_y = 2[B^2 + 2AC + 2^{1/2}kB(A - C)]$$

The values of A, B, and C are determined to solve the above three equations by using the anisotropic g values. In this calculation the value of k is fixed to 0.9. Since we cannot experimentally determine the sign of the observed g values, it is necessary to try many assignments to solve the equation. The reasonable solution is selected and listed in Table II. The fact that the value of B_1 is largest indicates that the ground-state Kramers doublet consists mainly of the state wherein the unpaired electron remains in the d_{xy} orbital and that the sign of the EFG is negative.

We choose the following Hamiltonian for the spin–orbit coupling and the crystal field distortion interactions:

$$\mathcal{H} = -\zeta\mathbf{l}\cdot\mathbf{s} - \delta(\mathbf{l}_z^2 - 2) - \frac{\epsilon}{2}(\mathbf{l}_+^2 + \mathbf{l}_-^2)$$

where δ and ϵ are tetragonal and orthorhombic distortion parameters, respectively. The ratios of δ/ζ and ϵ/ζ may be determined by using the values of A_1, B_1, and C_1. The values obtained are summarized in Table II.

(d) Temperature Dependence of the Quadrupole Splitting for the Spin-Crossover System. The temperature dependence of the quadrupole splitting (TQS) for a low-spin iron(III) has been examined.[28,29] The idea is discussed on the basis of the assumption that an iron atom is surrounded tetragonally with isotropic covalent bondings. The parameters A_i, B_i, C_i, and E_i/ζ are obtained by using the experimental anisotropic g values. The TQS can be expressed for the low-spin iron(III) system as follows, because quadrupole splitting ΔE_Q is defined as $^1/_2e^2QV_{zz}$ for axial symmetry:

$$\Delta E_Q = \frac{\sum_i \Delta E_{Qi} \exp(-E_i/kT)}{\sum_i \exp(-E_i/kT)}$$

$$\Delta E_{Qi} = {}^2/_7 e^2Q'\langle r^{-3}\rangle(s_i^2 + t_i^2)^{1/2} \qquad s_i = B_i^2 - {}^1/_2(A_i^2 + C_i^2)$$

$$t_i = 3^{1/2}A_i\cdot C_i$$

(28) Golding, R. M. *Mol. Phys.* **1967**, *12*, 13.
(29) Schmidt, J. G.; Brey, W. S., Jr.; Stoufer, R. C. *Inorg. Chem.* **1967**, *6*, 268.

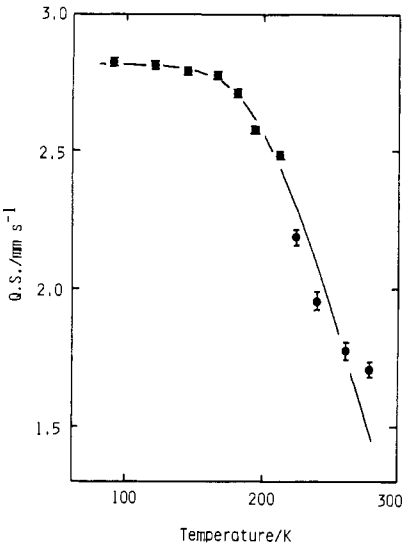

Figure 11. Temperature dependence of the quadrupole splitting for [Fe(acen)(dpp)](BPh$_4$). The solid line has been calculated with the parameters listed in Table III.

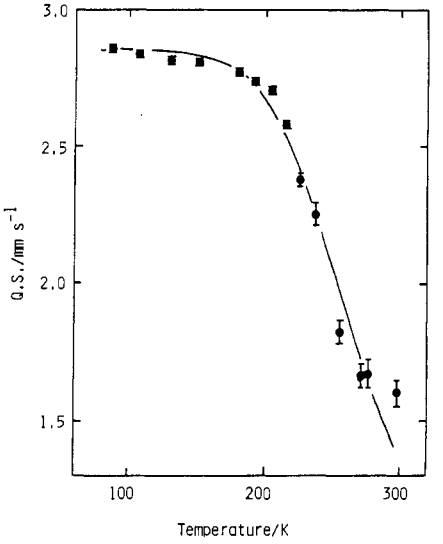

Figure 12. Temperature dependence of the quadrupole splitting for [Fe(acen)(pic)$_2$](BPh$_4$). The solid line has been calculated with the parameters listed in Table III.

Table III. Best-Fit Parameters in the Calculation of the TQS for Spin-Crossover Iron(III) Complexes

complex	E_Q(lat),[a] mm s^{-1}	E,[b] cm^{-1}	ζ,[c] cm^{-1}
[Fe(acen)(dpp)](BPh$_4$)	0.310	330	227
[Fe(acen)(γ-pic)$_2$](BPh$_4$)	0.347	339	250

[a] Temperature-independent contribution of the quadrupole splitting. [b] The separation between zero-point levels of the two states. [c] One-electron spin–orbit coupling constant.

where $e^2Q'\langle r^{-3}\rangle$ is estimated to be 8.9 mm s^{-1}.[28] This equation can be modified to describe the TQS of the spin-crossover system having a rapid electronic relaxation time.

For a ^6A–^2T system, the TQS is given by

$$\Delta E_Q = \frac{\sum_i \Delta E_{Qi} \exp(-E_i/kT)}{\sum_i \exp(-E_i/kT) + 3C\exp(-E/kT)}$$

where C is the ratio of the molecular vibrational partition functions[23] in the two spin states obtained by the magnetic susceptibility measurement and E is the separation between

the zero-point levels of the two spin states. The quadrapole splitting is composed of the sum of ΔE_{val} and ΔE_{lat}; the subscript "val" refers to the contribution from the charge distribution of the aspherical "3d-valence" electron and the subscript "lat" from the charge distribution of the neighboring ions in the crystalline lattice. If the component of ΔE_{lat} in the ^6A state is assumed to be the same as that in the ^2T state in this calculation, the parameters are obtained as shown in Table III. Figures 11 and 12 show the plots of the experimental data of the quadrupole splitting together with the theoretical curves that are obtained by using the best parameters listed in Table III. These values evaluated from the TQS by the least-squares method are reliable rather than those from the temperature dependence of the effective magnetic moment, because we have neglected the distortion of the crystal field in the process of calculating the theoretical temperature dependence of the effective magnetic moment. However, not much significance is attached to this value, because there is a fair latitude in the choice of C; that is, C is defined to be constant in this calculation in spite of the fact that C may be in general dependent on temperature.

The ligand field parameters and crossover parameters for the rapid electronic relaxation of the spin-crossover system calculated in this study are similar to those for the slow electronic relaxation. The rates of $^2T \rightleftarrows {}^6A$ spin interconversion take place as fast as 10^{-7} s, although these electron transfer accompanied by changes in spin multiplicity, therefore, are spin-forbidden transitions ($\Delta s = 2$). The electron transfer must proceed through the ligand orbitals, and the interaction of an iron atom with lattice vibrations will play an important role. Furthermore, it is important that π-conjugation is involved in the chemical structure and the ligand is stereochemically flexible.

Conclusion

The Mössbauer absorption spectra for the spin-crossover iron(III) complexes showed the rapid electronic relaxation phenomena between ^6A and ^2T states. It is notable that the behavior of $[Fe(acen)(lut)_2](BPh_4)$ is different from that of the other complexes in the electronic relaxation time in spite of its similar thermodynamic data. The introduction of a methyl group in the 2-position of pyridine results in steric hindrance, leading to the inhibition of the ligand molecule motion, and changes the electron density at the iron atom. The steric hindrance affects the coupling between the spin transition and lattice vibration and thus may cause the different electronic relaxation time according to the stereochemical structure of each complex.

Registry No. $[Fe(acen)(dpp)](BPh_4)$, 83555-99-1; $[Fe(acen)(pic)_2](BPh_4)$, 62660-72-4; $[Fe(acen)(lut)_2](BPh_4)$, 86507-81-5.

Contribution from the Department of Chemistry, University of Texas, Austin, Texas 78712

Electrochemistry in Liquid Sulfur Dioxide. 4. Electrochemical Production of Highly Oxidized Forms of Ferrocene, Decamethylferrocene, and Iron Bis(tris(1-pyrazolyl)borate)[1]

PAUL R. SHARP[2] and ALLEN J. BARD*

Received November 17, 1982

The electrochemistry of $Fe(C_5H_5)_2^+$, $Fe(C_5Me_5)_2^+$, and $Fe(HB(pz)_3)_2^+$ (pz = pyrazolyl) in liquid SO_2 was investigated. All three species show one oxidation wave and one reduction wave corresponding to production of the 2+ and neutral forms, respectively. While $Fe(C_5H_5)_2^+$ is stable in SO_2, the 2+ form reacts to block the electrode surface. For $Fe(C_5Me_5)_2$ and $Fe(HB(pz)_3)_2$ both the 1+ and 2+ forms are stable on the coulometric time scale. The neutral forms react with the solvent to generate the 1+ forms. Electrochemical data and visible absorption spectra, for $Fe(C_5Me_5)_2^{2+}$ and $Fe(HB(pz)_3)_2^{2+}$, and magnetic susceptibility results, for $Fe(C_5Me_5)_2^{2+}$, are reported.

Introduction

In a previous paper we showed that liquid SO_2 is a useful solvent for the generation and study of highly oxidized transition-metal complexes.[1] In this paper we report the first observation of the two-electron-oxidation product of ferrocene, $Fe(C_5H_5)_2^{2+}$ (**1**), electrochemically generated in SO_2. In addition, stable solutions of the permethylated analogue, $Fe(C_5Me_5)_2^{2+}$ (**2**), and the related pyrazolyl borate complex $Fe(HB(pz)_3)_2^{2+}$ (**3**) have been obtained and characterized. While electrochemical oxidation of $Fe(C_5Me_5)_2$ to the 2+ form in $AlCl_3$/1-butylpyridinium chloride melts has been reported previously, under similar conditions $Fe(C_5H_5)_2^+$ was oxidized in a multiple-electron irreversible process.[3] The 2+ form of $Fe(HB(pz)_3)_2$ has not been previously reported. Our electrochemical studies suggest a closer relation (at least electronically) of the $HB(pz)_3$ ligand with the C_5Me_5 ligand rather than the previously proposed analogy with the unsubstituted C_5H_5 ligand.[4]

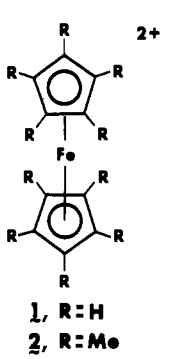

1, R = H
2, R = Me

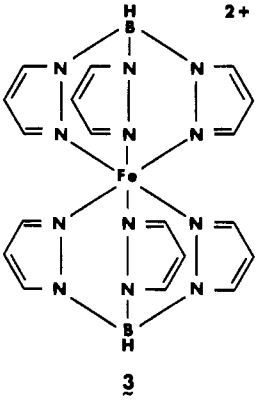

3

Experimental Section

Electrochemical studies were performed in conventional single- and three-compartment cells by using previously reported procedures.[1,5]

(1) For part 3 in this series see: Gaudiello, J. G.; Sharp, P. R.; Bard A. J. *J. Am. Chem. Soc.* **1982**, *104*, 6373–6377.
(2) Present address: Department of Chemistry, University of Missouri at Columbia, Columbia, MO 65211.
(3) Gale, R. J.; Singh, P. *J. Organomet. Chem.* **1980**, *199*, C44–C46.
(4) Trofimenko, S. *J. Am. Chem. Soc.* **1967**, *89*, 3904–3905.

0020-1669/83/1322-2689$01.50/0